# Dynamical exponents for the current-induced percolation transition in high-$T_c$ superconductors

Mladen Prester
*Institute of Physics of the University, P.O. Box 304, HR-10 000, Zagreb, Croatia*
(Received 31 October 1995; revised manuscript received 6 March 1996)

A detailed study of dissipation in weak link networks of high-$T_c$ superconductors has been performed. The model for dissipation has been elaborated assuming a general correspondence with the problems of inhomogeneous charge transport. The model treats the basic experimental ingredients, current-voltage ($I$-$V$) and current-differential resistance ($I$-$dV/dI$) characteristics, as a current-induced critical phenomenon. The validity of a simple relationship between non-Ohmic weak link network and Ohmic classical percolation networks has been proved, allowing a quantitative interpretation of $I$-$V$ characteristics. These characteristics are primary determined by dynamical features of transport on percolation networks. The model focuses on both aspects of of the scaling-related power law, its dynamical exponent and its prefactor, and gives specific predictions for magnetic field and temperature dependencies. The experimental results are in full agreement with both predictions. In particular, the experimental values of dynamical scaling exponents ($t=2$, $s=0.7$) coincide with generally accepted literature values for three-dimensional systems. [S0163-1829(96)01826-7]

## I. INTRODUCTION

The effect of structural inhomogeneities on transport properties of cuprate high-$T_c$ superconductors (HTS), although extensively studied by a number of authors,[1] is still not fully understood yet. The term *inhomogeneities* applies here both to intrinsic deviations from the average crystallographic structure (such as variation of the local structure or the oxygen stoichiometry on the length scale of the unit cell) and to extrinsic microstructural features (such as grain boundary[2] weak links on $\mu$m scale). In this work we concentrate on the latter, i.e., the weak link aspect of inhomogeneities, primarily on the weak link networks (WLN) which characterize a variety of forms of realistic samples. There are many reasons for interest in transport properties of weak-link-dominated samples. Besides general interest in studying the phenomenon of superconductivity in cuprates, there are several specific reasons. First, a detailed understanding of the mechanisms which underlie the onset of dissipation and the concept of critical current itself is equally important for both fundamental physics and for the intended practical applications. Secondly, these samples represent, primarily due to intrinsically short coherence length[3,4] of HTS, an ideal granular superconductor. This is a system which has attracted, together with Josephson-junction arrays,[5] a lot of attention in the past decades,[6] in particular due to the fact that the questions of long range order (or of the phase coherence) in these heterogeneous systems correspond to quite general problems of critical phenomena.[7,8]

The latter aspect will be thoroughly investigated by this work. In particular, we show that the problem of charge transport in WLN can be considered within the framework of transport in heterogeneous media, i.e., as the problem of dynamics of percolation (or fractal) networks.[7,8] In several recent publications[9–11] we presented some experimental arguments which support this approach and demonstrate the problem of dissipation in HTS, as studied by current-voltage ($I$-$V$), current-differential resistance ($I$-$dV/dI$), and temperature-resistance ($T$-$R$) characteristics, to be basically in agreement with the predictions of classical percolation theory. In this paper we establish a still missing model appropriate for analysis of charge transport in WLN and the related current-induced percolation transition. The model is then applied to the interpretation of new experimental findings in investigated $I$-$V$ and $I$-$dV/dI$ characteristics both in ranges of varying temperatures and varying (small) magnetic fields. The level of agreement between the predictions of the model and the experimental data leads us to recognize the polycrystalline HTS, a WLN prototype, as a rather unique model system for experimental studies of dynamical scaling exponents of current-induced percolation transition, interpreted as a critical phenomenon. Also, as a final argument for the importance of studies of transport in WLN, we point out that a relatively simple problem of transport in WLN may serve as a starting model for more complex (or more intrinsic) problems. For example, there are indications[12] that the global vortex motion in the flux lattice may be subject to similar macroscopic constraints as those present in WLN. The similarity of the power-law $I$-$V$ characteristics of the two different systems may be therefore attributed to the common constraints, and not to the details of the microscopic mechanisms. In Sec. II we first introduce the basic physics of Josephson coupled systems, then list some relevant results which appropriately focus the problem of dissipation in WLN of HTS and finally elaborate the model for nondissipative and dissipative transport itself. Section III deals with quantitative analysis of experiments and their relevance for the investigation of dynamical features on percolation clusters. Section IV specifies the region of fractal growth within which the present model cannot be applied. The analytical proof for an expression linking an Ohmic and a non-Ohmic network, the latter comprising two elementary junction's types, is elaborated in the Appendix.

## II. MODEL FOR DISSIPATIVE AND NONDISSIPATIVE TRANSPORT IN WEAK LINK NETWORKS

### A. Weak link network as a granular superconductor

The mechanism of Josephson coupling has been invoked in order to explain the bulk superconductivity in high-

 

temperature superconductors in both cases of the intrinsic interplane ($CuO_2$) coupling[13] and the coupling across microstructural objects (grain boundaries, oxygen depleted regions, etc.).[3,4] The transport properties of Josephson-coupled system depend on the specific parameters of the problem. In particular, the properties of the systems under consideration, polycrystalline samples of HTS, are determined by competing effects between the three characteristic energies: the energy of intergranular Josephson coupling $E_J$, the energy of thermal disorder $E_T$, and the electrostatic charging energy $E_C$.[14] The granular character of transport in these systems is a consequence, along with the short coherence,[3] of these competing energies.[4] The latter two are detrimental for the Josephson-coupled phase which can therefore be realized only if the characteristic parameters of a given superconductor allow sufficiently strong $E_J$.[15] More specifically, it turns out that the temperature at which $E_J$ exceeds $E_T$ lies close below $T_c$, the critical temperature of the intragranular thermodynamic phase transition, while the charging energy $E_C$ remains low enough (primarily due to relatively large average grain sizes[15]), thus allowing a sufficiently strong phase coupling. The important fact is that the long range phase coherence may be drastically influenced by the parameters imposed externally (applied current, magnetic field and temperature), leaving simultaneously the intragranular superconductor in its Meissner state.

### B. Some experimental features of dissipation in WLN

Distinct and separable dissipative contributions belonging either to superconducting grains or to the system of their interconnections, WLN, can be identified in various types of transport measurements[16] (ac susceptibility, dc magnetization, voltage noise). Also, there is a broad experimental range of temperature, applied current and/or magnetic field inside which the dissipative excitations (whatever their nature) are localized exclusively in WLN.[17,9] It has been firmly established that precisely these localized excitations are responsible for the experimental $I$-$V$ characteristics of bulk samples.[9] No quantitative agreement with flux-creep ($V \propto e^{J/J_c}$, $J$ being the applied current density and $J_c$ the characteristic current) or flux-flow regime ($R_f \propto H/H_{c2}$, with $R_f$ defined below) could be detected in these measurements. In the experimental window of our measurements these classical dissipative processes may therefore be neglected.[18] We recall here some results which prove that the localized excitations make a discrete set, being limited in its total number of elements only by microstructure of the polycrystalline samples.[9] In other words the experimental arguments listed below confirm the existence of a network in its conventional sense.

(i) There is a sample-dependent quasi-Ohmic high current saturation level of $I$-$V$ characteristics, $R_f$. $R_f$ is systematically smaller than $R_n$, the normal resistance just above the transition ($R_f = 0.2R_n$ typically) and has a very weak magnetic field and temperature dependence.

(ii) There is a pronounced branching in a set of $R$-$T$ characteristics[11] (resistive transition curves taken by measuring currents inside a wide range). The position of the branching point coincides[9] with $R_f$.

(iii) $R_f$ and the branching point systematically depend only on microstructure of the samples.[9]

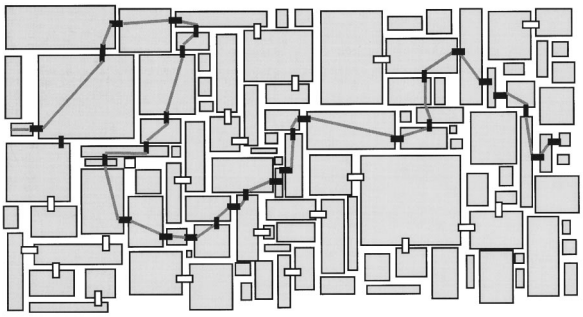

FIG. 1. Schematic view of supercurrent transport in non-Ohmic WLN of HTS. Phase coherent grains (disordered rectangles) are interconnected by junctions in one of the two possible states, *black* (supercurrent *on*) or *white* (supercurrent *off*). The conductive status of a junction is determined by local conditions.

(iv) The onset of dissipation is best described by a power law, provided the applied current $I$ is replaced by the reduced current[9] $i = I - I_c$, $I_c$ being the critical current. The scaling is characterized by a sample- (i.e., microstructure) independent exponent.[19,9] The exponent also reveals no temperature and magnetic field (if $H < 20$ Oe) dependence.

These observations [(i)–(iv)] make a starting point for the model presented below which treats the onset and growth of dissipation in WLN, composed of a large but final number of elements, as a problem of heterogeneous conducting medium (e.g., random resistor network[7]) and its well-understood dynamical features. In particular, we model the WLN as a system composed of grains in the Meissner state, interconnected with the switching devices (Josephson junctions) in one of the two possible conducting states[20] (supercurrent ''on'' or ''off''). The status of a particular junction responds to the local conditions, i.e., the local values of current, magnetic field, and temperature. The supercurrent transport in the model medium is illustrated schematically in Fig. 1.

### C. Growth of percolation cluster in classical and weak link networks

The model for dissipation follows in essence the knowledge of transport in electrically conducting random networks. The representative examples[7] are random resistor networks (RRN) and random superconductor networks (RSN) in which a fraction of originally isolating (RRN) or normally conducting (RSN) sites (bonds) are randomly replaced by conducting or superconducting sites (bonds), respectively. The (better) conducting fraction will be hereafter designated as $p$. As it is well known, the resistance $R$ of both networks follows the power-law (scaling) behavior close to the percolation threshold $p_c$,

$$R \propto |p - p_c|^n. \tag{1}$$

This relationship applies to RRN with $n \equiv -t$ (for $p > p_c$) and to RSN with $n \equiv s$ (for $p < p_c$), respectively. The dynamical exponents $t$ and $s$, which describe divergence of $R$ *above* $p_c$ (RRN) or its vanishing *below* $p_c$ (RSN), Fig. 2, have been thoroughly studied during the past decades[7,8] for two-dimensional (2D) and 3D systems. Their values are known to be $t \approx 2$ and $s \approx 0.7$ in 3D. In order to make the

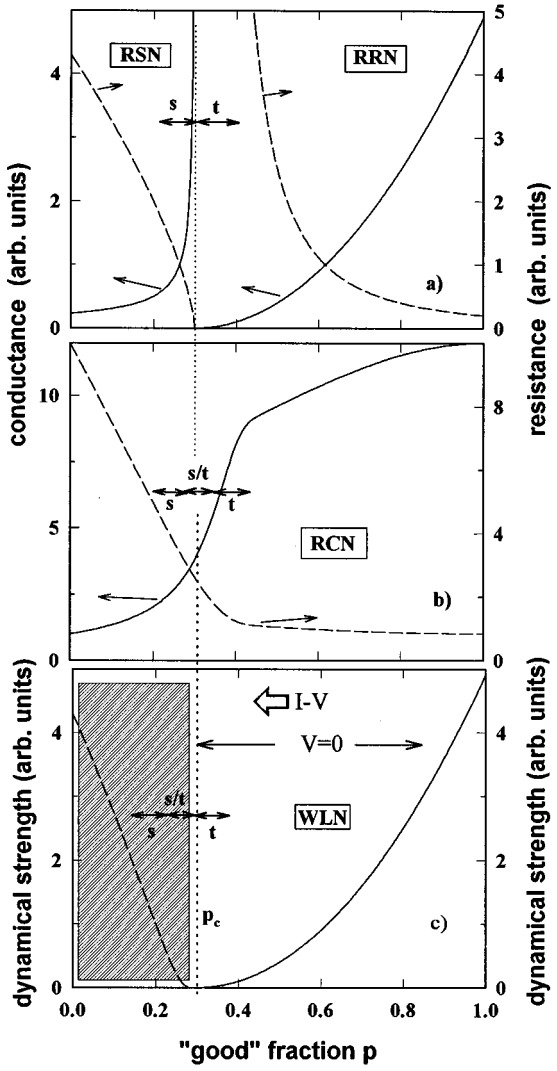


FIG. 2. Power-law resistance and conductance of classical percolation Ohmic networks close to the percolation threshold $p_c$ of better-conducting (*good*) fraction $p$. Illustration concerns 3D case so the assumed values of dynamical exponents were $t=2$ and $s=0.7$, respectively. In (a) the characteristic behavior of random resistor and random superconductor network was shown while (b) models a random composite network. The components of the latter network are both normally conducting but the respective values of their conductivities differ substantially. The regions characterized by $s$- and $t$-like cluster dynamics or their crossover are marked by $s$, $t$, or $s/t$, respectively. (c) illustrates the behavior of *dynamical strength* of infinite cluster in WLN (see text) which is nonzero in the zero-voltage region of $p$. Thick arrow indicates the direction of variation of $p$ which corresponds to increasing current branch of experimental $I$-$V$ characteristics. Dissipative part of these characteristics, the subject of this study, corresponds to hatched region of (c). The characteristic cluster dynamics are marked as in (b).

model more complete and realistic we also introduce the problem of prefactor of this power law. The prefactor $R_t$ should tell how the total resistance scales with the resistance of dissipative elements at the lattice sites $r_0$ and with the size $L$ of a sample. In $d$-dimensional space $R_t$ scales as[7,21]

$$R_t=\left(\frac{l}{L}\right)^{d-2} r_0, \tag{2}$$

where $l$ is a size of the network unit cell. Therefore, the resistance $R$ of the network (or its conductance $G$) reads now

$$R=1/G=\left(\frac{l}{L}\right)^{d-2} r_0|p-p_c|^n. \tag{3}$$

It is important to stress that the above expressions are valid only in the approximation of a very large system ($L\to\infty$). For a real system of finite size there is always a crossover value $p^*$, close enough to $p_c$, below which the diverging correlation length $\xi$ ($\xi\propto|p-p_c|^{-\nu}$) approaches the sample size, $L\approx\xi$, and a finite-size scaling takes over.[7] Inside the interval $(p_c,p^*)$ a sample-sized cluster becomes a fractal with non-Euclidean dimension $d_f$, $d_f\neq d$, and Eqs. (1)–(3) are not obeyed.[7] However, as shown in the discussion section, the experimental conditions of this report are in most cases compatible with $L\gg\xi$, i.e., with the percolation regime of Eqs. (1)–(3). Due to the reality of a large sample limit in the experiments we report on, the term ''sample-sized cluster'' will be replaced by ''infinite cluster'' in the remaining text. It is also important to note, in accordance with the experimental results listed previously, that $R_t$ is represented by $R_f$ in measurements on real HTS samples. A growth of the (super)conducting clusters in RRN or RSN which accompanies the rise of (super)conducting fraction $p$ is usually studied either numerically or, as in some experiments,[22] by physical manipulation with the composition of the samples. It is assumed here that there is a similar cluster growth in WLN. The growth is related to current-induced variation of the relative number of supercurrent carrying links. The WLN system is self-organized in the sense that its composition as well as the spatial configurations of property-bearing clusters are regulated by current itself. The normalized number of ''good'' links in WLN, which obviously plays the same role as $p$ in RRN and RSN, may be represented as an unknown function of the applied current, magnetic field, and temperature, $p=p(I,H,T)$. The specific functional form of $p$ may be sample dependent following the specific features of an actual Josephson network, including the microstructure of a given sample. Here we only assume that, owing to disorder, this function is nonsingular in its variables.

It can be expected that the behavior of the WLN system is quantitatively related to the bond percolation problem of some hypothetical RRN or RSN image network (in the Appendix we call it ''an Ohmic counterpart of WLN''). In order to justify this connection we first carefully examine the problem of involved scaling exponents.

#### *1. Two specific dynamics on percolation cluster: Exponents t and s*

The dynamical exponents $t$ and $s$ in Eqs. (1)–(3) express two different dynamics in the two (RRN,RSN) networks: In the terminology of diffusion on a percolating network,[23] the dynamical exponent $s$ is associated with a random walker (''termite'') which performs a normal random walk when off the superconducting cluster but which moves extremely rapidly when on the cluster. In contrast, the dynamical exponent $t$ represents ''the dynamics of an ant''[24] which executes a normal random walk only on the percolation cluster. In other words the exponent $t$ is associated with dynamics exclusively on the conducting cluster in its isolating background

(i.e., there is no distribution of current between two subsystems, the incipient cluster and the background), while $s$ applies to the case of current being distributed between the superconducting and normally conducting clusters. The two exponents are exactly equal in $d=2$ ($s=t=1.23$), but the strict relationship for higher dimensions has not been firmly established yet.[7,8] The third type of random network which is of interest here is a random composite network[25,26] (RCN). It allows the study of dynamical features both below and above the percolation threshold. This network comprises two types of resistive elements differing significantly [but not qualitatively as in RR(S)N cases] in relative values of their resistances. There are two regions of concentration $p$ where either $s$ or $t$ dominates the behavior of global resistance of RCN,[25] as well as an intermediate interval of $p$ around $p_c$ inside which a matching of $s$- and $t$-like dynamics takes place; see Fig. 2. The presence of cluster dynamics on *both* sides of $p_c$ in this network is the primary reason why we find it important for the interpretation of the onset of dissipation in WLN. Both in RRN and RSN the dynamical features in the region below (RRN) or above (RSN) $p_c$, respectively, cannot be a subject to resistance (or conductance) measurements due to the presence of an infinite cluster for all $p$ there. This cluster eliminates (in RRN) or shunts out (in RSN) any voltage on the sample of the network. To this extent it is instructive to decompose the expression for conductance, Eq. (3), into two factors, i.e., the geometry and sample dependent network factor $\mathcal{NF}$, $\mathcal{NF}=(L/l)^{d-2}g_0$, and the dynamical factor $\mathcal{D}$, $\mathcal{D}=|p-p_c|^{-n}$. In analogy with the conceptually related static quantity, the probability of an arbitrary site belonging to the infinite cluster, sometimes also called the cluster *strength*,[27] $\mathcal{D}$ may be called *the dynamical strength.* Unlike statical strength, $\mathcal{D}$ depends only on the backbone mass of the infinite cluster,[28,7,8] the dead ends mass being irrelevant for global conduction. The advantage of $\mathcal{D}$ is that it can be introduced, in order to characterize the dynamical features on an infinite cluster, in the ranges of $p$ inside which the observables are zero or infinite. In particular, it is important to consider $\mathcal{D}$ of RSN (Ref. 29) in the range $p>p_c$. This range is characterized by a trivial shunting effect ($V=0$) due to infinite conductance $g_0$ of the network elements (i.e., $\mathcal{NF}=\infty$) and corresponds to the nondissipative branch of the $I$-$V$ characteristic of WLN. The dynamical strength of an infinite (also phase-coherent) cluster is at its maximum inside that range for a network without a normal fraction ($p=1$) and drops to $\mathcal{D}=0$ with decreasing $p$ (increasing $I$ in WLN) at $p_c^+$, a breaking point of infinite cluster [see Fig. 2(c)]. The specific dynamics which accompanies the disappearance of $\mathcal{D}$ can be inferred by noting the formal similarity with dynamics in RRN: The supercurrent bypasses a resistive site in RSN (or an off site in WLN) in the same way, i.e., without any local branching, as the normal current does in RRN around isolating sites. Therefore the problem of $\mathcal{D}$ is formally identical, for $p\to p_c^+$, to the problem of vanishing $G$ in RRN. The value of the exponent $n$ in the expression for $\mathcal{D}$ is accordingly $n=-t$. The relevant dynamics actually involves, above but close to $p_c$, only a backbone of an infinite cluster[7,8,28] and will be hereafter called *a t-like* dynamics. We propose that the same $t$-like dynamics underlies the dynamical strength $\mathcal{D}$ of WLN (RSN) for $p>p_c^+$ as well.

#### *2. Cluster dynamics of the dissipation onset in WLN*

We analyze now the excursion of $p$ through $p_c$, following the route $p^+\to p_c^-$ and below when the dissipation sets in. In RRN some of the most critical (*red*[28,7]) links in the backbone become isolating during this course and the global conduction as well as the backbone's dynamical strength ceases. In WLN some of the red links become dissipative, the global phase coherence disappears and the voltage sets in. Due to the insertion of this dissipative ''glue'' the dynamical strength recovers and can be identified, owing to its partially dissipative character for $p<p_c$), with $R$. The associated cluster dynamics may be inferred from the following consideration. First, it is clear that at the very onset of dissipation there could be no ''explosion'' in the number of dissipative sites as the scaling power lower than 1, e.g., $s=0.7$ would imply. Moreover, as the dissipative sites are still tied to the backbone it turns out that the very onset should be characterized by a $t$-like dynamics as well so that $\mathcal{D}$ is expected to be symmetric around $p_c$ in a small interval of $p$ around $p_c$. More precisely, there is an onset, at $p_c^-$, of a crossover from backbone related $t$-like dynamics to dynamics which activates not only the dangling ends of the largest cluster but also all other disconnected clusters. This sort of cluster dynamics will be hereafter called *an s-like* dynamics. We note that the same type of crossover was studied in RCN a long time ago;[25] see Fig. 2. The only difference is that in RSN-related WLN the crossover interval of $p$ is not symmetric around $p_c$ like in RCN but rather sets in just at $p_c$. Our reasoning concerns primarily the problem of WLN analyzed here as a bond RSN problem. We are not certain, however, whether our conclusion that the very onset of dissipation is determined by a $t$-like dynamics could be applied to RSN in general.

### D. Quantitative formulation of the model and its main assumptions

In this work we are mainly interested in experimental $I$-$V$ characteristics, i.e., the continuous reduction of $p$ by increasing current $I$, usually in a fixed magnetic field $H$ and temperature $T$. As long as $p>p_c$ there is an infinite phase coherent cluster in WLN and no voltage can be measured along the sample. Below $p_c$ a dissipative voltage sets in. The $I$-$V$ characteristic can be viewed as a possible scenario for the experimental path of the point $p(I,T,H)$ in the four-dimensional $p$-$I$-$T$-$H$ space ($T$ and $H$ are fixed parameters and $p$ changes due to varying current $I$). The dissipation sets in at the dissipation onset curve, $p(I,H,T)=p_c$, regardless of the previous history of the working point $p(I,T,H)$. In order to simplify the presentation, the further treatment of the function $p$ is going to include two variables only, e.g., $p=p(I,H)$. The explicit treatment of the third variable ($T$) would lead to the same qualitative behavior. Even in the two-variable case the full reconstruction of function $p(I,H)$ (a surface in the 3D system of coordinates $I,H,p$) from experiments seems still too ambitious. A precise reconstruction of the function $p(I,H,T)$ is outside the scope of this work. Instead, it rather relies on the function's general analytical properties which can be deduced by physical reasoning: Due to the broad statistical distribution of several relevant parameters characterizing the samples (grain and sample size, junc-

tions' quality, etc.) but regardless of the width of this distribution for fixed $T$ and $H$, the function $p(I,T,H)$ is a monotonously decreasing function of the increasing current $I$. We first ask about the curves of constant $p$ in the $I$-$H$ plane, $p(I,H)=$const. These must be some nonlinearly decreasing $I=I(H)$ functions. For example, two reasonable assumptions would be $I=ae^{-bH}$ and $I=a/(H+b)$, where $a,b$ are parameters. These functions could serve as reasonable test functions as they are both ''mesoscopically'' justified: the first one due to the magnetic field dependence of critical currents of superconductor–normal-metal–superconductor (SNS) junctions,[30] and the second one due to the sample-size effects in critical currents.[31] The function of constant $p$ in these two cases would be of the form $p=Ie^{bH}$ and $p=I(H+b)$, respectively, with the dissipation onset curves given by the equation $p(I,H)=p_c$. In order to proceed with the quantitative formulation of the model it is necessary to introduce some assumptions, primarily about the unknown function $p(I,H)$. These assumptions are as follows.

(i) Critical current $I_c$ is the current consistent with the percolation threshold $p_c$, $p(I_c)=p_c$.

(ii) The function $p(I,H)$ is linear in $I$ close to $I_c$. In its quantitative aspect the model is therefore restricted to the small current interval around $I_c$ inside which a linear approach is permitted.

(iii) The dependencies on $I$ and $H$ can be factored out, $p(I,H)=f(I)g(H)$. [In previous examples $f(I)=I$ and $g(H)=e^{bH}$ or $(H+b)$, respectively.] The function $f(I)$ allows more complicated forms of current dependence of $p$ than the oversimplified linear one. The magnetic field dependent critical current is defined by $p[I_c(H)]=f(I_c)g(H)=p_c$.

(iv) Quantity $R$ of linear percolation networks has to be replaced by $dV/dI$ (differential resistance) of nonlinear WLN. Due to non-Ohmicity the resistance $R(=V/I)$, which is a well-defined macroscopic observable of Ohmic systems (RRN,RSN), fails to play the same role in WLN. The analogy between the two quantities, $R$ and $dV/dI$, was justified by qualitative arguments in Ref. 10. In Appendix this is proven analytically for two representative networks.

The dynamical state of WLN stems from the difference $p(I,H)-p_c$. In the vicinity of $I_c$ the linear expansion gives

$$p-p_c=\left(\frac{df}{dI}\right)_{I_c} g(H)[I-I_c(H)] =(c_2/c_1)[p_c/I_c(H)][I-I_c(H)], \tag{4}$$

In order to make the model more tractable we introduced here the coefficient $c_1$ of the line which joins the origin and the point $f(I_c)$ on $f(I)$ curve such that $f(I_c)=c_1I_c$ (see inset to Fig. 8), or $I_c(H)=p_c/[c_1(H)g(H)]$. The slope of $f(I)$ at $I_c(H)$ is designated in Eq. (4) as $c_2$. If the function $f(I)$ were linear the factor $c_2/c_1$ of the current curve $f(I)$, hereafter called *a shape factor* (see inset to Fig. 8), would be equal to one. This factor is field and sample dependent and responsible, together with $p_c/I_c(H)$, for the field dependence of the experimental power-law prefactor. By virtue of transformation $R\leftrightarrow dV/dI$ from Eq. (3) and using Eq. (4) we get

$$dV/dI=1/G=R_t|p-p_c|^n =\left(\frac{l}{L}\right)^{d-2} r_0[c_2g(H)]^n[I-I_c(H)]^n \tag{5}$$

or

$$dV/dI=R_f(c_2/c_1)^n p_c^n(I/I_c-1)^n =R_f(c_2/c_1)^n[p_c/I_c(H)]^n[I-I_c(H)]^n. \tag{6}$$

The voltage in the measurements of $I$-$V$ characteristics should therefore follow:

$$V=\int (dV/dI)dI=\frac{R_f}{n+1}(c_2/c_1)^n(p_c/I_c)^n(I-I_c)^{n+1}. \tag{7}$$

In these equations the total resistance $R_t$ of a network was replaced by its WLN counterpart, $R_f$. The notation of these expressions suggests explicitly the conditions of fixed magnetic field. Qualitatively, there would be no differences if the conditions of fixed temperature were assumed and in this case we may simply replace $H$ by $T$. The basic agreement of the experimental $I$-$V$ (and $I$-$dV/dI$) characteristic with a power-law form has already been demonstrated.[9,10] The value of the exponent $n$ at the very onset of dissipation has been preliminary identified as $n=t$. In this work we report, besides the details of the model as presented above and in the Appendix, on the full experimental confirmation of the validity of Eqs. (5)–(7) for the interpretation of experimental characteristics. In particular, we show that the relatively complex structure of the power-law prefactor indeed contains the dependences on all environmental conditions of the measurements (magnetic field, temperature) and on the specific properties of the samples, while the exponent depends only on cluster dynamics and therefore remains insensitive until the crossover to the alternate dynamical regime takes place. In the remaining part of the article we quantitatively test the predictions of the model.

## III. QUANTITATIVE ANALYSIS OF $I$-$V$ AND $I$-$dV/dI$ CHARACTERISTICS

### A. Samples

The properties we report on in this work concern the weak link networks of HTS in general, i.e., the properties under considerations are not related to some specific preparative conditions. Three samples chosen for presentation belong to two families of HTS, $R\mathrm{Ba_2Cu_3O_{7-x}}$ ($R$ is a rare earth element) and $\mathrm{Bi_2Sr_2Ca_2Cu_3O_{10+y}}$. The rare earth was either gadolinium (sample $S_1$, also GBCO) or yttrium (sample $S_2$, also YBCO). Sample $S_3$ was a lead-substituted compound $\mathrm{(BiPb)_2Sr_2Ca_2Cu_3O_{10+y}}$ (BPSCCO). The preparations followed a conventional mixture-of-powders route and the details are given in references mentioned in Table I. This table also gives a summary of some of the transport properties of the samples.

TABLE I. Some transport and microstructural properties of the samples. $\varrho_{RT}$ and $R_{RT}$ are room-temperature resistivity and measured resistance of the sample, respectively. $\varrho_{at}$ is resistivity just above the transition and $T_{c0}$ temperature of zero resistance. $\langle a \rangle$ is the average grain size of the samples and $J_c$ critical current density measured at specified temperatures.

| | $S_1$, GBCO[a] | $S_2$, YBCO | $S_3$, BPSCCO[b] |
|---|---|---|---|
| $\varrho_{RT}$ [$\mu\Omega$ cm] | 980 | 1700 | 4860 |
| $R_{RT}$ [m$\Omega$] | 45 | 57 | 185 |
| $T_{c0}$ [K] | 93.5 | 90 | 104 |
| $\varrho_{at}$ [$\mu\Omega$ cm] | 420 | 745 | 2830 |
| $R_f$ [m$\Omega$] | 6.9 | 4.5 | 15.8 |
| $\langle a \rangle$ [$\mu$m] | 8 | 35 | 20 |
| $J_c$ [A cm$^{-2}$] | 17 (88 K) | 80 (80 K) | 25 (80 K) |

[a]For preparative details see Ref. 9.
[b]For preparative details see Ref. 10.

### B. Data representation and power-law exponent

There may be different ways of representing compatibility of experimental curves with the form of power law. One way would be a straightforward fit to the power-law form of Eqs. (5)–(7). This fit would have three parameters ($I_c$, $n$, and a prefactor), too much for a convincing determination of their values. It is also very common to plot the experimental $(V,I)$ points on the logarithmic axes so that the slope of the linear part, if any, gives the exponent value. In this work we study the analytical properties of the experimental curves by a slightly different method. The voltages $V$ (or $dV/dI$) of the measured $I$-$V$ (or $I$-$dV/dI$) curves were first transformed following $V \rightarrow V^{1/n}$, where $n$ is a trial exponent value, and subsequently plotted versus the measuring current. The assumed power-law form of $I$-$V$ (or $I$-$dV/dI$) characteristic corresponds to the linear behavior of the transformed data and its slope to the power-law prefactor. There are no fitting parameters in this form of data presentation. With a suitable choice of $n$ we were able to detect, in numerous samples investigated so far, two linear (i.e., power-law) regimes, a trivial nondissipative ($I<I_c$) one and a dissipative one, crossing each other at the critical current $I_c$; see Fig. 3. It turns out, however, that there is an interval of values of $n$, Fig. 4, inside which any $n$ seems to lead, at first glance, to an acceptable fit to the power law. Therefore the proper exponent had to be determined therefore by quantitative tests of the quality of fits for several values of $n$ in this interval, as shown in Fig. 5. The mean-square deviation from the average straight line of the transformed and normalized $I$-$V$ (or $I$-$dV/dI$) data has been calculated for all of the chosen values of $n$. Figure 6 shows the general forms of these standard deviations as functions of trial values $n$ for samples in zero or very small applied magnetic fields. These functions are characterized generally by the presence of a minimum, both in the measurements of $I$-$V$ and $I$-$dV/dI$ curves. The best choice for exponent $n$ is, by definition, a value which minimizes the standard deviation. The high resolution measurements of $dV/dI$ on sample $S_1$, shown in Fig. 6 give $n \approx 2.1$. Similarly, the measurements of $I$-$V$ curves in the range of initial dissipation in sample $S_2$, Fig. 6, give $n+1 \approx 3$, i.e., $n \approx 2$. Within our model the exponent $n$ is interpreted as the dynamical exponent for conductivity $t$, so these experiments

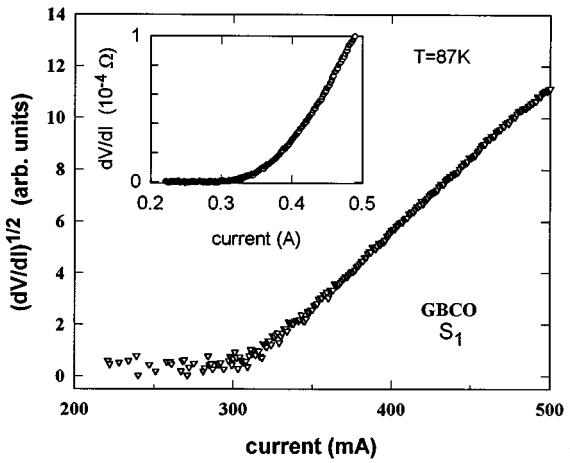


FIG. 3. Typical $I$-$dV/dI$ characteristics of polycrystalline HTS sample. The measured points (inset) are transformed following $dV/dI \rightarrow (dV/dI)^{1/n}$, $n=2$, to demonstrate consistency with the power-law behavior.

strongly favor $t \approx 2$. This result for $t$ is in good agreement with numerical results[7] on R(S)RN and the theoretical estimates of its lower[8] and upper[21] bounds.

The values of $n$ determined by a procedure like that were experimentally found to be almost insensitive either to temperature changes inside a broad interval (66–90 K) and variation of magnetic fields (if $H<20$ Oe) or to the choice of the family of the sample and its microstructure. The absence of such dependences is in a full accordance with the principles of our model: Dynamics remains unchanged regardless of the level of the $T$- and $H$-dependent rate of creation of isolating/dissipative bonds, taking place in increasing current.

### C. Power-law prefactor and the consistency of the model

The prefactor of the power law in Eqs. (5) and (6), hereafter denoted as $P_f$, is a product of three factors, viz., the

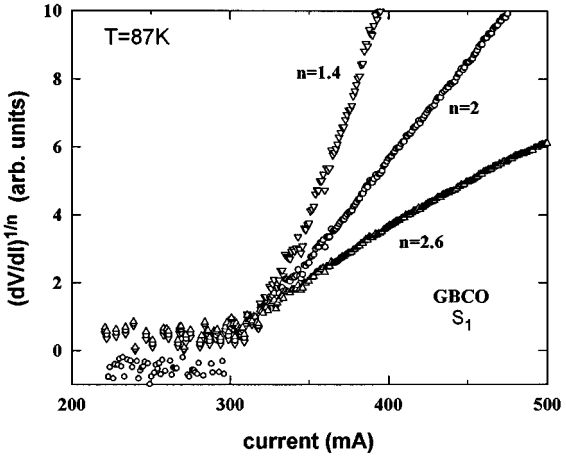


FIG. 4. Transformed $dV/dI$ data of the measurement from Fig. 3 for three trial values of $n$. The proper choice, obviously close to $n=2$, would give a straight line. The other two give either concave-downward ($n=2.6$) or concave-upward ($n=1.4$) shapes of transformed curves.

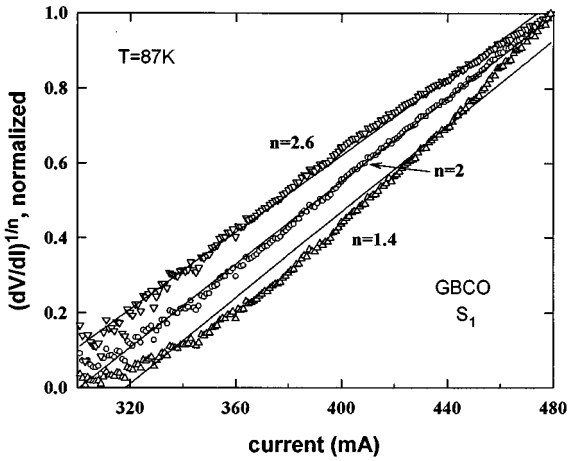


FIG. 5. Transformed $dV/dI$ data, normalized by their values at 480 mA, for three trial values of $n$ (open symbols) and the best fits to straight line (solid lines). Quantitative analysis is shown in Fig. 6.

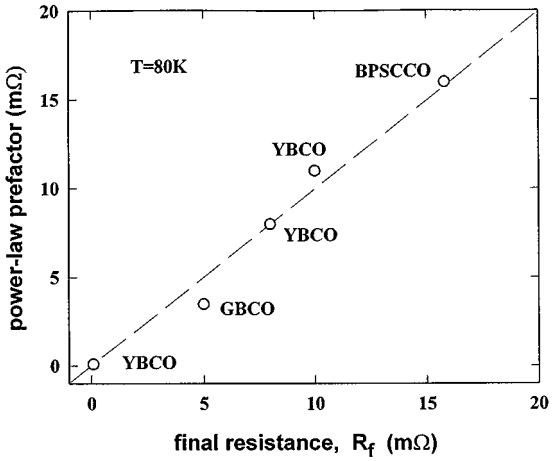


FIG. 7. Correlation of power-law prefactor values and final resistance (see text) for several samples of different batches and origins.

total resistance $R_f$, the shape factor $(c_2/c_1)^n$ of the current function $f(I)$ at $I_c$, and the critical current factor $(p_c/I_c(H,T))^n$. While $R_f$ has a very weak dependence on magnetic field and temperature, the shape factor and especially the critical current factor are strongly $H$ and $T$ dependent. In this model $c_2/c_1$ is in a simple geometrical relationship (see inset to Fig. 8) with the *a priori* unknown function $f(I)$. The spectrum of realistic values for $c_2/c_1$ can, however, be easily determined. If we assume for example that $f(I)$ is a power-law function of $I$ around $I_c$, allowing a large range for its power $r$ (from concave-downward functions, $r<1$, to concave-upward functions, $r>1$), it follows from the definition of $c_2/c_1$ that it is simply equal to $r$. Therefore it is reasonable to expect that the temperature and magnetic field dependent values of $c_2/c_1$ fall into the interval not broader than [0,10] at most. It is also important to note that $c_2/c_1$ is the main representative of the effects of disorder so that sample dependence of the shape factor can be also expected. We first demonstrate qualitatively (i.e., without taking explicitly into account the shape factor and the critical current factor) the correlation of $P_f$ with $R_f$. Figure 7 shows the collective prefactor data at 80 K for several HTS samples of various families and microstructures, shown as a function of $R_f$. The variation of $R_f$ in these samples is a well-understood[9] consequence of different average grain sizes $\langle a \rangle$. The latter quantity can be treated as an effective spatial coarseness of WLN network, playing therefore the role of $l$ in Eqs. (2), (3), and (5) thus determining $R_f$ and, in turn, $P_f$. However, a full quantitative determination of $P_f$ depends also on $(c_2/c_1)^n$ and $(p_c/I_c)^n$. In our model these factors are solely responsible for temperature and magnetic field dependences of $P_f$. Before investigating these predicted dependences of $P_f$, it is important to test the mutual consistency, within the proposed model, of experimental results for $n$ and $P_f$. In the system of data presentation used in this study, to each value of the trial power-law exponent $n$ we may associate one experimental value for $P_f$. $P_f$ may be geometrically represented by the slope $S$ of the line which fits the transformed data. In terms of experimental observables, the model predicts a simple relationship between the slope $S$ and the total resistance $R_f$,

$$S=(c_2/c_1)(p_c/V_mI_c)R_f^{1/n}, \tag{8}$$

where $V_m$ is the voltage (or differential resistance) used for data normalization. It is only $c_2/c_1$ in this formula which is not known experimentally. $R_f$ can be determined in an independent $I$-$V$ measurement, while $I_c$ is known from the $I$-$V^{1/n}$ presentation of the experimental $I$-$V$ (and $I$-$dV/dI$) data. The numerical test we present has also to assume some choice for the unknown percolation threshold concentration

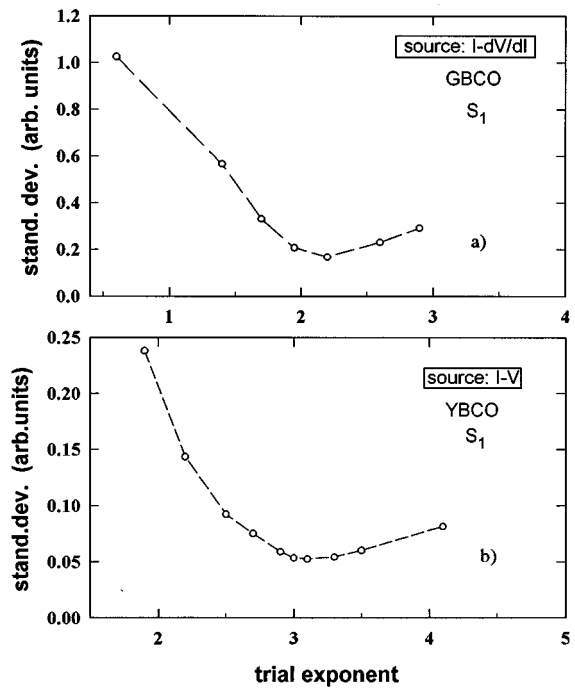


FIG. 6. Mean square deviation of transformed and normalized data from the best fit to the straight line, for various trial exponent values. (a) illustrates the result for $I$-$dV/dI$ and (b) for and $I$-$V$ measurements. The exponent value in the center of the pronounced minima is in excellent quantitative agreement with literature data for the conductivity exponent $t$ in 3D.

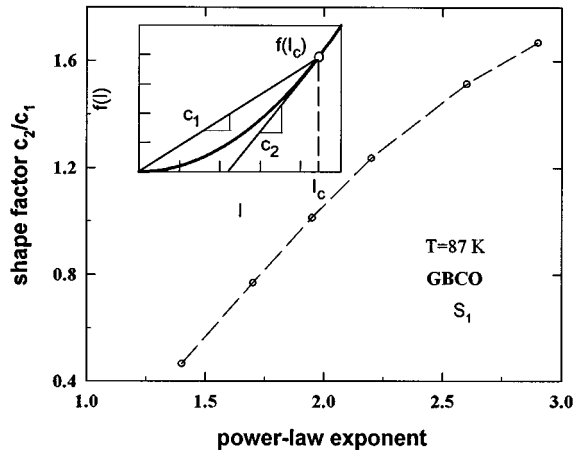


FIG. 8. Dependence of the calculated shape factor $c_2/c_1$ on trial exponent values from Fig. 6(a). Inset: Graphical meaning of the shape factor. $c_2$ and $c_1$ are coefficients of the two characteristic lines associated with the point on the current function $f(I)$.

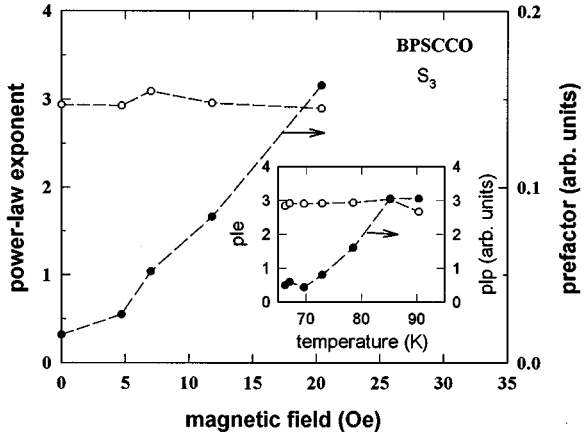


FIG. 9. Magnetic field dependence of power-law exponent (ple) and power-law prefactor (plp) determined from measurements of $I$-$V$ characteristics of sample $S_3$. Corresponding temperature dependence is shown in the inset. Dashed lines are guides for the eye only.

$p_c$. Here we use $p_c$ of the 3D cubic (bcc) bond problem,[7,8] i.e., $p_c \approx 0.18$. The real $p_c$ of our problem can of course differ from 0.18 but this would introduce only a slight numerical difference into the results. Now, the necessary condition for the consistency of the model is that the shape factor $c_2/c_1$ should acquire a reasonable value, i.e., a value inside the interval [0,10]. In Fig. 8 we show the values for $c_2/c_1$, for several exponents $n$, calculated from Eq. (8) and from the values for $S$, $I_c$, $V_m$, and $R_f$ taken from the measurement at 88 K. It is obvious that all of the calculated $c_2/c_1$ fall into the expected interval. The proper value of $c_2/c_1$ (at the given conditions of measurement, $H=0$ Oe, $T=88$ K) is the one associated to proper $n$. Figure 8 suggests therefore that $c_2/c_1=1$ (compatible with $n=t=2.1$). In other words, the values of $c_2/c_1$ smaller than 1, as well as those much higher than 1 are excluded due to the same quantitative arguments which favor $n=t=2.1$. Furthermore, the value of $c_2/c_1$ much higher than 1 already at 88 K is increasingly improbable due to the fact that by decreasing temperature $c_2/c_1$ monotonically increases, starting from some value $c_2/c_1<1$ (below but close to $T_c$). A typical value of $c_2/c_1$ at 78 K is $c_2/c_1=5$ (see the inset to Fig. 11). It can be concluded therefore that there are no basic inconsistencies in our model.

### D. Power-law prefactor and dependences on $H$ and $T$

The physical origin of dependences on magnetic field ($H$) and temperature ($T$) comes, to the first order, simply from the $H$- and $T$-dependent critical current of disordered individual Josephson junctions of WLN. This is then reflected into $H$- and $T$-dependent fraction of dissipative elements $p(I)$ which introduces also the corresponding dependences of the global critical current $I_c$ and the shape factor $c_2/c_1$ of the current function $f(I)$, thus of the prefactor $P_f$ as well. The sensitivity of $P_f$ to the changes of $H$ and $T$ contrasts the experimental findings for scaling exponent $n$. According to the model, the exponent is related solely to the cluster dynamics, exhibiting therefore basically no $H$ and $T$ dependence, in full agreement with experimental results on sample $S_3$, shown in Fig. 9. Figure 10 illustrates the temperature variation of $P_f$ of the same sample, together with the variation of the quantity $(p_c/I_c)^n$ $(n=2)$. A dependence of the shape factor $c_2/c_1$ is also displayed. The latter quantity decreases almost linearly with increasing temperature but remains strictly inside the predicted interval of its values, [0,10]. The magnetic field dependence of the same quantities for sample $S_2$ is shown in Fig. 11. Again, $c_2/c_1$ displays a remarkable decrease in increasing magnetic field, still inside the same interval. We note that the specific functional dependences of $c_2/c_1$ vary from sample to sample, which allows somewhat different $c_2/c_1$ values at the same temperature and magnetic field for different samples. It is also interesting to note that the approximate cancelation of $p_c/I_c$ and $c_2/c_1$ is quite common to occur at 80 K, so that the effective prefactor values of $P_f$ are numerically close to $R_f$ at that temperature. This is also a reason which justifies, *a posteriori*, the slope of the straight line in Fig. 7.

### E. Crossover of dynamical exponents in increasing magnetic fields

The voltage which sets in at $I_c$ is primary determined, in our model, by the characteristic dynamics represented by the

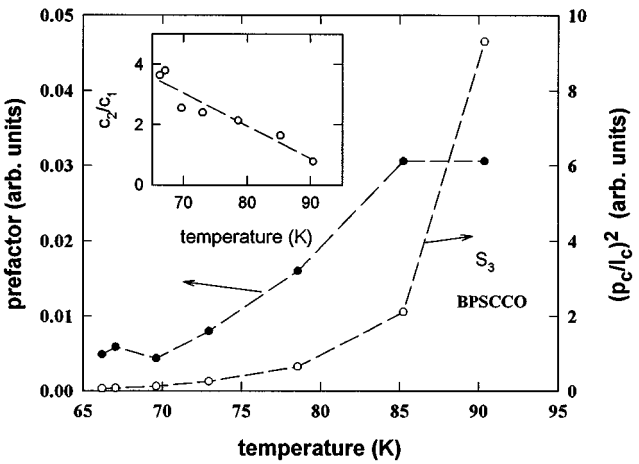


FIG. 10. Temperature dependence of power-law prefactor and two of its factors predicted by this model, $(p_c/I_c)^n$, $n=2$, and $c_2/c_1$ (inset), for sample $S_3$. Dashed lines are guides for the eye only.

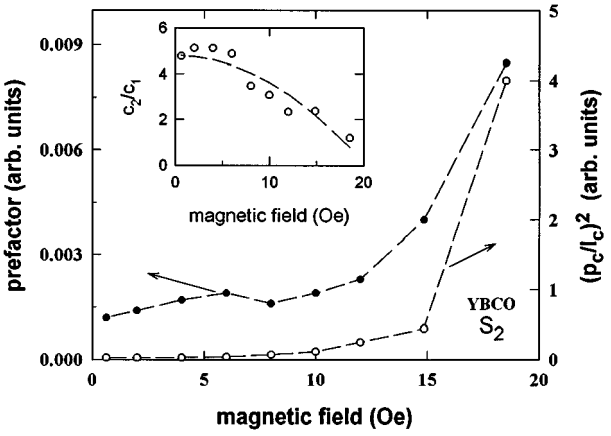


FIG. 11. Magnetic field dependence of power-law prefactor and two of its factors predicted by this model, $(p_c/I_c)^n$, $n=2$, and $c_2/c_1$ (inset), for sample $S_2$. Dashed lines are guides for the eye only.

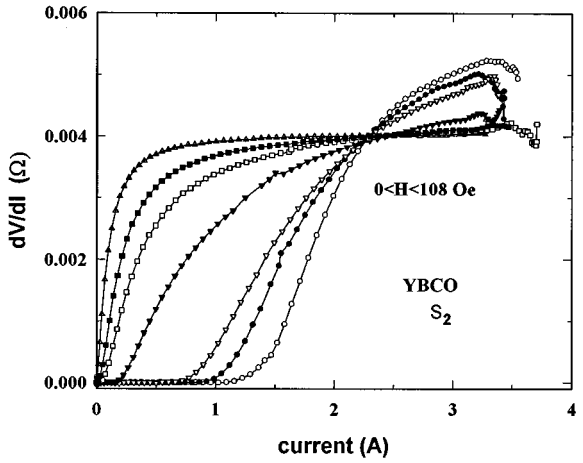


FIG. 12. Typical $I$-$dV/dI$ characteristics in a broad range of applied currents and in various magnetic fields, sample $S_2$. Somewhat decreasing level of quasi-Ohmic saturation for high currents in increasing magnetic field was referred to as *final resistance* $R_f$ in text.

exponent $t$. The model also predicts a possible crossover to another type of cluster dynamics, i.e., to the dynamics described by the dynamical exponent $s$. In the latter case the model predicts the rise of differential voltage still in the form of Eqs. (5) and (6), but with $n$ equal to $n=s=0.7$ instead of $n=t=2$. In order to investigate the possibility of this crossover we studied the $I$-$dV/dI$ characteristics of sintered YBCO in a broad range of applied currents, i.e., up to the currents which produce a voltage much above the range of initial dissipation. In the broad range of currents one can expect, according to our model, the fingerprints of three consecutive regimes. The first two should reflect a crossover from $t$-like $[dV/dI\sim(p-p_c)^t]$ to $s$-like $[dV/dI\sim(p-p_c)^s]$ cluster dynamics while the third regime, very far from $I_c$ (i.e., $p_c$), has nothing to do with critical behavior and reflects a linear conductance-concentration dependence in the effective medium theory of heterogeneous systems[32] $(dV/dI\sim p)$. [It is important to note that the exact forms of $f(I)$ and $g(H)$ are limited therefore by the boundary condition on $p$, i.e., $p(I\rightarrow\infty,H)=1$.] This makes a basis of our analysis of $I$-$dV/dI$ curves in a broad range of applied currents. The generic $S$ shape is a well-known feature of these characteristics; see Fig. 12. We have already reported[10] a qualitative agreement with the crossover prediction in the absence of applied field. Here we report on the sequence of measurements in varying magnetic fields. Figure 12 shows a set of $I$-$dV/dI$ characteristics which all saturate at some characteristic value $R_f$. A slight $R_f(H)$ dependence can be attributed to second-order effects (partial flux trapping inside the grains[33]). Each of these curves was numerically analyzed in the two regions of currents, just above $I_c$ (hereafter the range of *small currents*) to study initial dissipation, and a subsequent range of currents much higher than the critical one (hereafter the range of *intermediate currents*) but still much smaller than the current in quasi-Ohmic saturation $dV/dI=R_f$. For small currents the best power-law exponent was found for each magnetic field in the investigated range ($H<20$ Oe) by looking for the standard deviation minimum (Fig. 6). This procedure gives the dynamic exponent values of $n=t\approx 2$ for all applied fields, with the usual $H$-dependent prefactor. The solid concave-upward curves in Fig. 13 are corresponding plots of $P_f(I-I_c)^t$. For intermediate currents the fraction $p$ of superconducting links is far away from $p_c$ and the validity of percolation power-law expressions like Eq. (1) is, *a priori*, not justified. Nevertheless, the model was tested in that range too by plotting the expected functional form $P_s(I-I_c)^{0.7}$ where we put $n=s=0.7$; see Fig. 13. $P_s$ is a fitting parameter and $I_c$ the same critical currents that had been used previously for small currents. There is obviously a good reproduction of experimental curves, proving at least qualitatively the relevance of $s$-like cluster dynamics in the intermediate range. In the third range of very large currents, inside which $I$-$dV/dI$ is close to saturation to $R_f$, it is reasonable to assume the validity of Maxwell's classical theory of conductivity in electrically heterogeneous media.[32] The latter (effective medium) approach applies when one fraction represents only a small perturbation to the other, dominant fraction, and resistivity $(\varrho)$ scales linearly with $p$, $\varrho\propto p$. In our case of WLN the range of large currents corresponds therefore to linear dependence of $dV/dI$ on $p$. In that region the plotted $I$-$dV/dI$ curves are directly proportional to $p(I)$. It is interesting to note that the fraction function $p(I)$, although still analytically unknown, is basically reconstructed in two current ranges: for small currents it is represented by $c_2/c_1$ and for large currents it is proportional simply to $dV/dI$. In order to investigate the crossover between the exponents more closely, it is instructive to study the magnetic field dependence of both $P_f(I-I_c)^t$ and $P_s(I-I_c)^s$ curves. One way would be an independent study of these curves as functions of magnetic field. A shortcut to the results of these studies may be performed by investigating the crossing point of the two curves. The crossing point (see Fig. 13) shifts systematically to the left in the increasing field. It can be immediately concluded that the prefactors have different dependences on $H$: If there were a common prefactor, say $P$, then the crossing point would have the coordinate $(I_c+1,P)$. This is in clear disagreement with the results, Fig. 13, which shows decreasing (instead of increasing) ordinate of the crossing point in growing $H$. Our model predicts specific structures of the prefactors, $P_s=R_f(c_2/c_1)^s(p_c/I_c)^s$ and $P_f=R_f(c_2/c_1)^t(p_c/I_c)^t$, respectively. The current that per-

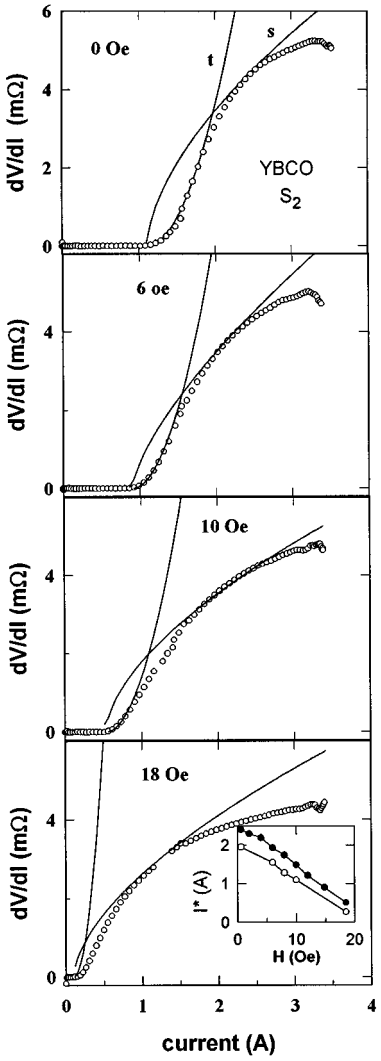


FIG. 13. Set of high-current $I$-$dV/dI$ characteristics in small magnetic fields and two relevant power laws (solid curves). The concave-upward curves were determined in the range of initial dissipation (approximately inside symbol size on this scale) and are consistent with $t$-like behavior. The concave-downward solid curves are the single-parameter ($P_s$) power-law fits, $P_s(I-I_c)^{0.7}$, intended to test a crossover to $s$-like dynamics, $s \approx 0.7$. The inset compares magnetic field dependence of the experimental (open symbols) and calculated position (black symbols) of the crossing point of these two power laws.

tains to crossing point, $I^*$, can be easily calculated to obtain, as a prediction of our model, the exponent-independent result $I^* = I_c[1+(c_1/c_2)(1/p_c)]$. The inset to Fig. 13 compares these calculated values for $I^*$ (using measured $I_c$ and earlier $c_2, c_1$ on the same sample; see inset to Fig. 11) with the experimentally determined $I^*$. Although there is not a full numerical agreement, a reasonably good reproduction of dependence on $H$ is obvious. This proves that the crossover range can be successfully described in both aspects of dynamical exponents and prefactors by the present model in spite of its clear limitations. The quantitative disagreement with the prediction of the model deserves some additional comments. Our measurements were taken until the chosen low-level voltage (10 $\mu$V), the same for all investigated $I$-$V$ characteristics from Fig. 4, has been reached. This voltage may correspond to various excitation levels, i.e., fractions of dissipative links $p'(I)$ above $p_c$ in the two measurements at different $T$ or $H$. For example at low temperature and in zero applied field the 10 $\mu$V criterion may provide a window of $p$ inside which the cluster dynamics is strictly governed by the dynamical exponent $t$ [concerning both the experimental exponent and the prefactor of $I$-$V$ (or $dV/dI$) curves]. At higher temperature and/or in higher field the same criterion does not necessarily warrant the presence of a single cluster dynamics. If there is some mixing of the two dynamics, then the prefactor, as well as the exponent, will not be determined by either of the derived expressions. This especially applies to the prefactor, because the effect on the exponent could be numerically too small to be effective. The latter scenario seems to be the most important reason that limits quantitatively the applicability of the simple expressions derived in the model. As far as the position of the crossing point is concerned we may conclude that a full quantitative agreement in a broad range of fields fails due to the ''mixing'' of the two prefactors in real $I$-$dV/dI$ characteristics. The position of the crossing point gives, however, a measure for relative contributions of the two types of cluster dynamics in different magnetic fields. Above 20 Oe the $s$-like dynamics is by far predominant, so that the detection of initial $t$-like behavior, although always present, is a matter of voltage resolution above $I_c$. Our interpretation of asymmetric $S$-shaped $I$-$dV/dI$ curves stems therefore from the crossover between the two types of cluster dynamics. The earlier interpretation (Ref. 34) of these curves was based on the notion of the distribution function of critical current density, $d^2V/dI^2$, and treated the role of disorder somewhat differently. While in the latter approach the disorder is *a source* of features in $I$-$dV/dI$ characteristics (in particular, their generic shapes), in this model disorder regulates mainly *the width* of non-Ohmic behavior, not the features themselves. The generic shapes of these characteristics are therefore related, in our view, to rather universal cluster dynamics and their crossover.

## IV. DISCUSSION AND CONCLUSION

The majority of equations pertaining to the present model [e.g., Eqs. (2), (3), and (5)] refer to the limit of infinite sample size.[7] Its validity questionable in principle and has to be tested taking into account the circumstances of an actual sample. As already mentioned in comments following Eq. (3) the sample size effects become important in close vicinity $\Delta p = |p^* - p_c|$ of $p_c$, where $p^*$ is a crossover concentration below which the sample size is smaller than the diverging correlation length. Inside $\Delta p$ the fractal nature of the cluster violates the predicted behavior. It remains therefore to estimate the experimental circumstances compatible with the $\Delta p$ (fractal) regime. Being satisfied with an order of magnitude precision we analyze the situation of a typical sample. The size of the sample $L$ belongs to the millimeter scale and that of the network unit cell $l$ to the micrometer (average grain size) scale, e.g., $L=1$ mm, $l=5$ $\mu$m. Thus $\Delta p = (l/L)^{1/\nu} = 2.38\times10^{-3}$, where $\nu$ is the correlation length exponent, $\nu=0.88$ in 3D. As the total number of resistive sites is of the order of the total number of grains $N_g$, i.e., $N_g = 8\times10^6$, the concentration interval $\Delta p$ above $p_c$ corre-

sponds to $1.9\times10^4$ links turned into ''off'' state. The important issue is the associated current interval. A typical current compatible with $p=1$ (i.e., differential resistance $R_f$) at 80 K is 5 A. In linear approximation $\Delta p$ corresponds therefore to $\Delta I=12$ mA. The latter is the current interval inside which the proposed scaling should be violated. The current resolution of the majority of our experiments was of the same order so that the possible presence of fractal dimension effects was averaged out inside a first few measuring points. It would be interesting to see whether the increased current resolution would be able to detect a real fractal regime.

In conclusion, we presented the model for dissipation in WLN and applied it to the interpretation of a large number of measurements on HTS samples in zero or small applied magnetic fields. The model treats the problem of dissipation as a current-induced critical phenomenon which involves two types of specific dynamics on the relevant percolation cluster. The application of the model leads to reasonable numerical agreement with the experiments.


## ACKNOWLEDGMENTS

I would like to thank K. Uzelac, Z. Vučić, E. Granato, and E. Babić for fruitful discussions. I am also grateful to D. Marinić-Todorović and A. Kuršumović of Energoinvest, Sarajevo and F. C. Matacotta and P. Nozar of ICTP, Trieste, for providing us with some samples. Skillful assistance in measurements of Z. Marohnić, D. Babić, and N. Biškup is also gratefully acknowledged.


## APPENDIX: CURRENT-VOLTAGE CHARACTERISTICS OF OHMIC AND NON-OHMIC NETWORKS

The purpose of this appendix is to relate the observable ''differential resistance'', $dV/dI$, of a non-Ohmic weak link network (WLN) to the observable ''resistance,'' $R=V/I$, of the Ohmic counterpart of WLN. By the WLN's Ohmic counterpart we mean a hypothetical random resistor or random superconductor network (RRN,RSN) identical to the non-Ohmic WLN in all details except that the fraction $p$ of the better-conducting component of this Ohmic network is independent on current. The variation of $R$ with $p$ in these Ohmic networks obeys a well-established power law, $R=A|p-p_c|^n$ ($n_{\mathrm{RRN}}=-t$, $n_{\mathrm{RSN}}=s$). Provided that the approximations of our model are fulfilled we show here quite generally that the characteristic dependence of the Ohmic network, $R=A(p_c-p)^r$, where the power $r$ can be now any real number, implies the same functional form of the differential resistance ($dV/dI$) of its non-Ohmic counterpart WLN, i.e.,

$$dV/dI=B(p_c-p)^r=B'(I-I_c)^r, \tag{A1}$$

where $A$, $B$ and $B'$ are mutually related but here unimportant constants.

We first reconstruct the shape of the $I$-$V$ characteristic of WLN from the assumed form, $R=A(p_c-p)^r$, valid in an Ohmic network. The $I$-$V$ diagrams of a network like that are represented by a family of lines with the slopes $k=A(p_c-p)^r$. The slope progressively changes as a function of increasing concentration $1-p$ of *blocked* sites (i.e., insulating or resistive). There is a quasicontinuum of these linear characteristics: The two adjacent ones represent the states which differ in their respective number $n$ of blocked sites by one; see Fig. 14. The fraction of blocked sites $1-p$ is obviously related to $n$ by $1-p=n/N$, where $N$ is total number of sites. In our model of current-induced percolation transition we infer the creation of blocked sites in WLN to the current itself. In other words, there is a distinct current increment $\Delta I$ that is necessary to change the number of blocked sites by one. $\Delta I$ induces a jump to the neighboring characteristic, i.e., to the characteristic of the slope $k(n)$ consistent with the increased number $n$. The corresponding voltage $V_{\mathrm{WLN}}$ is determined by the characteristic $k(n)$ as long as the increasing current stays below $\Delta I$. When the current increment reaches $\Delta I$ again a jump to characteristic $k(n+1)$

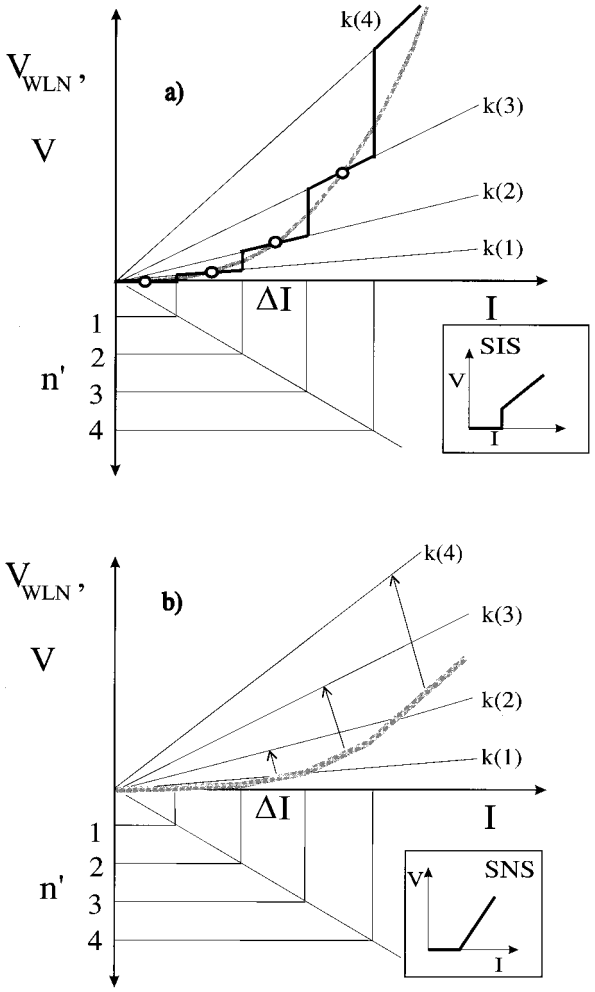


FIG. 14. Schematic reconstruction of $I$-$V_{\mathrm{WLN}}$ curves of weak link network from its linear counterpart, random resistor or random superconductor network. $I$-$V$ characteristics of the latter networks are straight lines of the slope $k$, shown here by thin lines as a function of the reduced number $n'=n-n_c$ of the insulating/resistive sites. The scheme of this figure illustrates the case of RSN. The voltage of non-Ohmic WLN network evolves in increasing applied current as a steplike curve, while the voltage measured experimentally follows, in a real situation with a quasicontinuum of states of different $n'$, the curve obtained by joining all the half-points (hatched line). (a) and (b) show the cases of two different junction types (insets), SIS and SNS. The $I$-$V$ curves in these two cases are both power laws with the common exponent, differing only in their prefactors.

takes place, and so on. The voltage of the $I$-$V$ characteristics of WLN represents therefore the curve obtained by movement of the working point from one characteristic to another. This curve depends however on the specific microscopic process responsible for ''jumps'' between characteristics. In our model this microscopic process is based on the features of individual Josephson junctions comprising the network. (We do not explicitly treat the other possible dissipative microscopic processes such as vortex-antivortex creation and movement, phase slips, etc., although we do not exclude the possibility that even in these cases the same global behavior could be expected[12]). To proceed we analyze the cases of the two representative networks composed of different junction types, superconductor-insulator-superconductor (SIS) and superconductor–normal-metal–superconductor (SNS), taking into account only the first-order $I$-$V$ nonlinearities of these junctions. The second-order effects (such as superimposed flux-creep/phase slip which gives some dissipation at any current, hysteresis, rounding at critical current and specific non-Ohmic behavior in the dissipative branch of junction's characteristics) are neglected in our model for global dissipation. The characteristics of the two junctions are therefore of the kind represented schematically in the insets to Fig. 14. We calculate now $V_{\mathrm{WLN}}$ and $dV_{\mathrm{WLN}}/dI$ as functions of current in these two cases.

#### 1. $I$-$V_{\mathrm{WLN}}$ and $I$-$dV_{\mathrm{WLN}}/dI$ for SIS network

The local SIS features lead to vertical switch of voltage [jump from the characteristic of the slope $k(n)$ to the adjacent one of the slope $k(n+1)$] at all current values that are multiples of $\Delta I$. In Fig. 14 we show schematically the very onset of dissipation which takes place when $n$ overcomes its percolation threshold value $n_c$, $n_c = p_c/N$. By $n'$ we designate here the reduced value of $n$, $n' = -n_c$. Therefore $n'=1$ corresponds to the status of the system in which the number of blocked sites exceeds $n_c$ by one. If the system were linear its $I$-$V$ characteristic in this state would be a line of the slope $k(1)$. For WLN and in the range of validity of the linear $p(I)$ approximation, $p = 1 - bI$, the status of the system evolves with increasing current as $n' = I/\Delta I$, while the voltage follows a steplike curve (heavy line in Fig. 14). The voltage measured in experiments is the envelope curve which joins all the half-way points. It is easy to show that the coordinates of these points are

$$\left( \frac{2n'+1}{2}\, k(n')\Delta I,\ \frac{2n'+1}{2}\, \Delta I \right). \tag{A2}$$

If we introduce the substitution $i = (n'+1/2)\Delta I$ [i.e., $n' = (i/\Delta I) - 1/2$] the voltage at the points is

$$V(i) = \frac{i}{\Delta I}\, k(n') = \frac{i}{\Delta I}\, k\left( \frac{i}{\Delta I} - 1/2 \right). \tag{A3}$$

The continuous function $V(I)$ (actually there is a quasicontinuum of states of different $n'$) that joins all the half-way points is therefore given by the transformation $i \to I$:

$$V(I) = \frac{I}{\Delta I}\, k(n') = \frac{I}{\Delta I}\, k\left( \frac{I}{\Delta I} - 1/2 \right). \tag{A4}$$

We are interested in the first derivative of this curve, the differential resistance $dV/dI$:

$$dV/dI = \frac{1}{\Delta I}\, k(n') + \frac{i}{\Delta I}\, \frac{dk}{dn'}\, \frac{1}{\Delta I}. \tag{A5}$$

The slopes are $k(p) = A(p_c - p)^r = A(1/N)^r (n - n_c)^r$, i.e., the slopes $k$ depend on $n'$ as the power law $k \sim (n')^r$. Taking into account that $I/\Delta I \gg 1/2$ and $dk/dn' = r(1/N)^r n'^{r-1}$, the differential resistance $dV/dI$ reads now

$$dV/dI = \frac{1}{\Delta I}\, k\left( \frac{I}{\Delta I} \right) + \frac{I}{\Delta I}\, \frac{A}{N^r}\, r(n')^{r-1}\, \frac{1}{\Delta I}. \tag{A6}$$

Keeping in mind that $n' = I/\Delta I$, we finally get the relationship we wanted to prove

$$dV/dI = \frac{1+r}{\Delta I}\, k\left( \frac{I}{\Delta I} \right) = \frac{1+r}{\Delta I}\, A(p_c - p)^r = B'(I - I_c)^r. \tag{A7}$$

We point out that this result relies upon a simple analytical property of power law functions $f(x) = x^r$, i.e., $[x/f(x)](df/dx) = r$. This expression actually holds for any homogeneous function. The corresponding expression is known as Euler's formula in mathematical literature. It is also interesting to note that a steplike voltage curve, quite similar to the heavy line in Fig. 14(a), has been obtained in the measurements of $I$-$V$ characteristics of artificial Josephson networks.[35] The relevance of our analysis for these results is, however, unclear at present.

#### 2. $I$-$V_{WLN}$ and $I$-$dV_{WLN}/dI$ for SNS network

If the local process belongs to the SNS type there will be no switches (voltages jumps) between adjacent characteristics of different $n$; see Fig. 14. It is instructive to follow the movement of the working point starting from a current just above $I_c$. This point initially follows, similarly as in previous SIS case, the characteristic $k(0)$. However, when the current overcomes the increment $\Delta I$ the slope changes from the initial $k(0) = 0$ to the slope $k(1)$, exhibiting at the same time no voltage jumps. The whole $I$-$V$ characteristic is therefore composed of linear segments the slopes of which are determined by the slopes of the characteristics $k(n')$. The proof of Eq. (A1) in this case is thus a straightforward consequence of the geometrical interpretation of the first derivative:

$$dV/dI = k(I/\Delta I) = A(p_c - p)^r = C(I - I_c)^r. \tag{A8}$$

We note that the two $I$-$V$ curves derived from elementary characteristics in these two cases are both power-law functions differing in their prefactors but sharing the same power law exponent.

[1] J. Halbritter, Phys. Rev. B **48**, 9735 (1993), and references therein.
[2] S. E. Babcock, MRS Bull. **8**, 20 (1992), and references therein.
[3] G. Deutscher, Physica C **153-155**, 15 (1988).
[4] J. R. Clem, Physica C **153-155**, 50 (1988).
[5] See, e.g., *Proceedings of the NATO Workshop on Coherence in Superconducting Networks*, edited by J. E. Mooij and G. B. J. Schön [Physica (Amsterdam) **B152** (1988)].
[6] See, e.g., *Inhomogeneous Superconductors-1979*, edited by D. U. Gubser, T. L. Francavilla, J. R. Leibowitz, and S. A. Wolf, AIP Conf. Proc. No. 58 (AIP, New York, 1980).
[7] D. Stauffer and A. Aharony, *Introduction to Percolation Theory* (Taylor and Francis, London, 1992); in *Fractals and Disordered Systems*, edited by A. Bunde and S. Havlin (Springer-Verlag, Berlin, 1991).
[8] T. Nakayama, K. Yakubo, and R. Orbach, Rev. Mod. Phys. **66**, 381 (1994).
[9] M. Prester, E. Babić, M. Stubičar, and P. Nozar, Phys. Rev. B **49**, 6967 (1994).
[10] M. Prester and Z. Marohnić, Phys. Rev. B **51**, 12 861 (1995); M. Prester, Physica C **235-240**, 3307 (1994).
[11] M. Prester and E. Babić, in *Proceedings of 7th Workshop on Critical Currents in Superconductors*, edited by H. W. Weber (World Scientific, Singapore, 1994), p. 521.
[12] M. Prester, in *Quantum Dynamics in Submicron Structures*, edited by H. A. Cerdeira, B. Kramer, and G. Schön (Kluwer Academic, Dordrecht, 1995), p. 645.
[13] R. Kleiner, F. Steinmeyer, G. Kunkel, and P. Müller, Phys. Rev. Lett. **68**, 2394 (1992).
[14] Y. Imry and M. Strongin, Phys. Rev. B **24**, 6353 (1981), and references therein.
[15] Y. Shapira and G. Deutscher, Phys. Rev. B **27**, 4463 (1983); A. Gerber, T. Grenet, M. Cyrot, and J. Beille, *ibid*. **43**, 12 935 (1991).
[16] S. Senoussi, J. Phys. III **2**, 104 (1992), and references therein.
[17] M. A. Dubson, S. T. Herbert, J. J. Calabrese, D. C. Harris, B. R. Patton, and J. C. Garland, Phys. Rev. Lett. **60**, 1061 (1988).
[18] We do not claim of course that there are absolutely no dissipative contributions at low current biases and in the range of ultrahigh (SQUID) voltage resolution due to, e.g., thermally activated flux creep of self-field-generated vortices. Our model applies to the 1–100 nV voltage resolution which is consistent with a perfectly defined critical current. The spatial organization of the dissipation which sets in above this current in macroscopic sample is focused by this work.
[19] E. Babić, M. Prester, D. Babić, P. Nozar, P. Stastny, and F. C. Matacotta, Solid State Commun. **80**, 855 (1991).
[20] M. Prester and Z. Marohnić, Phys. Rev. B **47**, 2801 (1993).
[21] D. B. Gingold and C. J. Lobb, Phys. Rev. B **42**, 8220 (1990).
[22] B. J. Last and D. J. Thouless, Phys. Rev. Lett. **27**, 1719 (1971); B. P. Watson and P. L. Leath, Phys. Rev. B **9**, 4893 (1974).
[23] P. G. deGennes, J. Phys. (Paris) Colloq. **41**, C3-17 (1980).
[24] S. Alexander and R. Orbach, J. Phys. (Paris) Lett. **43**, L625 (1982); Y. Gefen, A. Aharony, and S. Orbach, Phys. Rev. Lett. **50**, 77 (1983).
[25] A. L. Efros and B. I. Shklovskii, Phys. Status Solidi B **78**, 475 (1976); J. P. Straley, Phys. Rev. B **15**, 5733 (1977).
[26] T. Ohtsuki and T. Keyes, J. Phys. A **17**, L559 (1984).
[27] See, e.g., D. Stauffer and A. Aharony's book in Ref. 7.
[28] H. E. Stanley, J. Phys. A **10**, L211 (1977).
[29] The identical composition of the two networks, RSN and WLN, suggests that their cluster dynamics should be closely related.
[30] T. Y. Hsiang and D. K. Finnemore, Phys. Rev. B **22**, 154 (1980).
[31] H. Koppé, Phys. Status Solidi **17**, K229 (1966).
[32] J. C. Maxwell, *A Treatise on Electricity and Magnetism* (Oxford University Press, Oxford, 1904), Vol. II.
[33] In increasing applied magnetic field there is an effect of *magnetic coalescence*: The dipole magnetic field of the flux trapped in some of the neighboring grains is directed opposite to the applied field at the common boundary. The local field value is therefore reduced and this particular boundary is temporarily excluded from the network (the microstructure effectively coarsened, $R_f$ reduced).
[34] E. Babić, M. Prester, N. Biskup, Z. Marohnić, and S. A. Siddiqi, Phys. Rev. B **41**, 6278 (1990).
[35] M. Giroud, O. Buisson, Y. Y. Wang, B. Pannetier, and D. Mailly, J. Low. Temp. Phys. **87**, 683 (1992).